Available online at www.sciencedirect.com
ScienceDirect
International Journal of Thermal Sciences 47 (2008) 875–885
International Journal of Thermal Sciences
www.elsevier.com/locate/ijts

Effects of non-uniform porosity on double diffusive natural convection in a porous cavity with partially permeable wall

Sevgi Akbal [a], Filiz Baytaş [b,*]

[a] *Çekmece Nuclear Research and Training Center, Turkey*
[b] *Istanbul Technical University, Institute of Energy, 34469 Maslak-Istanbul, Turkey*

Received 15 September 2006; received in revised form 21 July 2007; accepted 23 July 2007

Available online 29 August 2007

Abstract

The double-diffusive natural convection in a porous cavity with partially permeable wall and with variable porosity was analysed by solving mass, momentum, energy and concentration balance equations, using Darcy's law. A cell-centred finite volume scheme was applied to solve the governing equations. Heat and mass transfer characteristics as isoconcentration lines, streamlines, isotherms, average Sherwood numbers and Nusselt numbers were studied for different values of Darcy modified Rayleigh number and porosity. The tests were performed at steady state using different sets of grids for numerical accuracy and stability.

Keywords: Non-uniform porosity; Cavity; Natural convection; Double-diffusivity; Darcy's Law; Finite volume

1. Introduction

Double-diffusive natural convection in porous media is mainly motivated by its importance in many natural and industrial problems. These include the disposal of waste material, groundwater contamination, chemical transport in packed-bed reactors, grain-storage installations, food processing, and drying process, the transport of a contaminant in saturated soil, the migration of moisture in fibrous insulation etc. The state of the art has been summarised very well in the literature authored by Nield and Bejan [1], Ingham and Pop [2] and Pop and Ingham [3]. The literature survey illustrates the extensive works that have been carried out on square, rectangular and shallow cavities with various wall boundary conditions.

An analytical and numerical study of natural convection heat and mass transfer through a vertical porous layer subjected to a concentration difference and a temperature difference in the horizontal direction has been studied by Trevisan and Bejan [4]. They used a two-dimensional rectangular porous medium, which its vertical walls were subjected to uniform fluxes of heat and mass while its horizontal walls were insulated and impermeable.

Many physical systems were modelled as a two-dimensional cavity with the vertical walls held at fixed but different temperatures or concentrations and the connecting horizontal walls considered as adiabatic or impermeable. Angirasa et al. [5] were reported a numerical study of combined heat and mass transfer by natural convection adjacent to vertical surfaces situated in fluid saturated porous media. They investigated numerical results for velocity, temperature and concentration at different Lewis and Rayleigh numbers.

Béghein et al. [6] have investigated natural convection in a square cavity filled with air mixed with different kinds of pollutants submitted to augmenting or opposing thermal and solutal gradients. The results showed that when the Lewis number is less than unity, the cavity is filled with a high diffusion pollutant. Akbal and Baytas [7] have investigated a radioactive gas transfer depending on the decay of the gas, Schmidt and concentration Grashof numbers by natural convection in a fluid saturated porous medium. The results indicated the gas concentration for different Schmidt and Grashof numbers strongly depends on the half-life of gas. Merkin and Mahmood [8] have investigated a model for the convective flow in a fluid-saturated

* Corresponding author. Fax: +90 212 2853884.
E-mail address: fbaytas@itu.edu.tr (F. Baytaş).

1290-0729/$ – see front matter
doi:10.1016/j.ijthermalsci.2007.07.007

Nomenclature

A	The ratio of impermeable part of the right wall, L_a/L	t	Time ..... s
C	Dimensional concentration ..... $\mathrm{kg\,m^{-3}}$	T_0	Reference temperature ..... K
C_0	Reference concentration ..... $\mathrm{kg\,m^{-3}}$	u, v	Velocity components in x and y directions . $\mathrm{m\,s^{-1}}$
C'''	Volumetric mass source strength in solid phase ..... $\mathrm{kg\,m^{-3}\,s^{-1}}$	U, V	Dimensionless velocity components in x and y directions
C^*	Dimensionless concentration	X, Y	Dimensionless Cartesian coordinates
D	Mass diffusivity ..... $\mathrm{m^2\,s^{-1}}$	x, y	Cartesian coordinates
g	Acceleration due to gravity ..... $\mathrm{m\,s^{-2}}$	*Greek symbols*	
k	Effective thermal conductivity of porous medium ..... $\mathrm{W\,m^{-1}\,K^{-1}}$	α	Thermal diffusivity ..... $\mathrm{m^2\,s^{-1}}$
K	Permeability of the porous medium ..... $\mathrm{m^2}$	β_C	Concentration expansion coefficient .... $\mathrm{m^3\,kg^{-1}}$
L	Cavity height ..... m	β_T	Thermal expansion coefficient ..... $\mathrm{K^{-1}}$
L_a	Height of impermeable part of the right wall .. m	ε	Porosity of the medium
Le	Lewis number, $\frac{\alpha}{D}$	θ	Dimensionless temperature
N	Buoyancy ratio, $\frac{\beta_C \Delta C}{\beta_T \Delta T}$	λ	General dependent variable
Nu	Average Nusselt number	ν	Kinematic viscosity ..... $\mathrm{m^2\,s^{-1}}$
q'''	Volumetric heat source strength in solid phase ..... $\mathrm{W\,m^{-3}}$	σ	Heat capacity ratio, $\frac{\varepsilon(\rho c_p)_f + (1-\varepsilon)(\rho c_p)_s}{(\rho c_p)_f}$
Ra	Darcy modified Ra number, $\frac{K g \beta_T L \Delta T}{\nu \alpha}$	ψ	Streamfunction
Sh	Average Sherwood number	Ψ	Dimensionless streamfunction
		τ	Dimensionless time

porous medium containing a reactive component. They considered the investigation in which the convective fluid within the porous material contains a reactive species, which reacts to form some inert product when in contact with impermeable wall.

Goyeau et al. [9] have studied the double diffusive natural convection using Darcy–Brinkman formulation in a porous cavity with impermeable boundaries, horizontal temperature and concentration differences. Bourich et al. [10] have studied a double diffusive natural convection in a square porous cavity submitted to cross gradients of heat and solute concentration numerically. Bahloul et al. [11] have investigated the double diffusive convection in a long vertical cavity heated from the below and imposed concentration gradient from the sides both analytically and numerically. Double diffusive steady natural convection in a vertical stack of square enclosures, with heat and mass diffusive walls, was studied numerically by Costa [12].

Recently, researchers' studies on heat and mass transfer in composite systems constitute a fluid and porous medium saturated with the same fluid. Gobin et al. [13] have focused on the simulation of double diffusive convective flows in a binary fluid, confined in a vertical enclosure, divided into two vertical layers, one porous and the other fluid. The combined heat and mass transfer rates for natural convection driven by the temperature and concentration gradients have been developed in a cavity containing fluid and porous layers by Singh et al. [14] and they showed that the degree of penetration of the fluid into porous region strongly depended upon the Darcy, thermal and solutal Rayleigh numbers.

The porosity has a significant impact in modeling the transport processes through porous media; the nature of porosity variation significantly affects heat transfer and fluid flow in the medium. The effect of variable porosity on natural convection in a packed-sphere cavity has been investigated numerically by David et al. [15] and they showed that in the conduction regime, variation of porosity lead to nonlinear temperature distributions. Saghir and Islam [16] have studied double diffusive phenomena in a layered porous bed with contrasting permeability.

The waste material storage is one of the samples of the porous media. The waste materials are generally stored in the impermeable cavities; the heat is generated in the cavity because of chemical reactions or nuclear decay heat and also the solid part of waste material in the cavity may produce radioactive gases because of nuclear decay. It is very important to prevent the leakage of the waste material from the cavity walls for environmental problems. The purpose of the present paper is considering the double diffusive natural convective flow in the two-dimensional fluid saturated porous cavity with heat and mass source in the solid phase. In this study, two main cases are taken into account. In the first main case, the cavity has a homogenous porosity in everywhere and in the other two main cases; the cavity has two regions with different porosity values. The left, upper and bottom walls of the cavity are impermeable and the right wall is partially permeable. The numerical results have been obtained by solving the Darcy, energy and concentration equations. This study focused on the effect of porosity and different Darcy modified Ra numbers on heat and mass transfer. As well as that it concentrates on the leakage of the partially permeable wall.

2. Mathematical modelling

The physical model and coordinate system are shown in Fig. 1. The cavity is cooled from all the walls. The right wall is partially permeable and other boundaries are impermeable as shown in Fig. 1. Soret and Dofour effects on heat and mass diffusion were neglected and Boussinesq approximation was held. According to Boussinesq's approximation, the density is assumed to be a linear function of temperature and concentration as follows:

$$\rho = \rho_0\left[1 - \beta_T(T - T_0) - \beta_C(C - C_0)\right] \tag{1}$$

where β_T and β_C are the coefficients for thermal and concentration expansion,

$$\beta_T = -\frac{1}{\rho_0}\left(\frac{\partial \rho}{\partial T}\right)_{P,C} \tag{2}$$

$$\beta_C = -\frac{1}{\rho_0}\left(\frac{\partial \rho}{\partial C}\right)_{P,T} \tag{3}$$

Also, the governing equations for mass, momentum (Darcy's law), energy and concentration can be expressed as follows:

$$\frac{\partial u}{\partial x} + \frac{\partial v}{\partial y} = 0 \tag{4}$$

$$\frac{\partial u}{\partial y} - \frac{\partial v}{\partial x} = -\frac{Kg\beta_T}{\nu}\left(\frac{\partial T}{\partial x} + \frac{\beta_C}{\beta_T}\frac{\partial C}{\partial x}\right) \tag{5}$$

$$\rho c_p\left(\sigma\frac{\partial T}{\partial t} + u\frac{\partial T}{\partial x} + v\frac{\partial T}{\partial y}\right) = k\left(\frac{\partial^2 T}{\partial x^2} + \frac{\partial^2 T}{\partial y^2}\right) + (1-\varepsilon)q''' \tag{6}$$

$$\varepsilon\frac{\partial C}{\partial t} + u\frac{\partial C}{\partial x} + v\frac{\partial C}{\partial y} = D\left(\frac{\partial^2 C}{\partial x^2} + \frac{\partial^2 C}{\partial y^2}\right) + (1-\varepsilon)C''' \tag{7}$$

The continuity equation is considered by defining a streamfunction $\psi(x, y)$, so that Eq. (5) can be written:

$$\frac{\partial^2 \psi}{\partial x^2} + \frac{\partial^2 \psi}{\partial y^2} = -\frac{Kg\beta_T}{\nu}\left(\frac{\partial T}{\partial x} + \frac{\beta_C}{\beta_T}\frac{\partial C}{\partial x}\right) \tag{8}$$

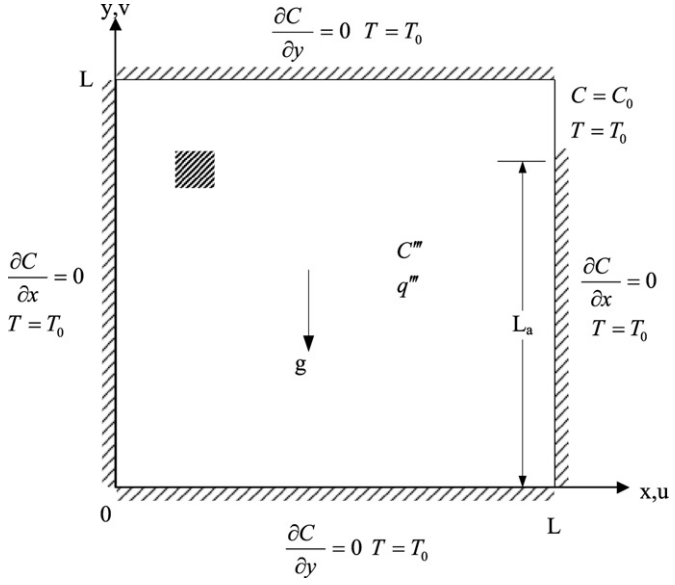

Fig. 1. Physical model and coordinate system for the porous cavity.

where $u = \partial\psi/\partial y$ and $v = -\partial\psi/\partial x$.

In this study, the following dimensionless variables are used for Eqs. (6), (7) and (8):

$$\Psi = \frac{\psi}{\alpha}; \quad X, Y = \frac{x, y}{L}; \quad U, V = \frac{u, v}{\alpha/L}$$

$$\tau = \frac{\alpha}{L^2}t; \quad \theta = \frac{T - T_0}{\Delta T}; \quad C^* = \frac{C - C_0}{\Delta C} \tag{9}$$

where $\Delta T = \frac{q'''L^2}{k}$ and $\Delta C = \frac{C'''L^2}{D}$.

Using these variables, the streamfunction, energy and concentration equations in non-dimensional form can be written as:

Table 1
Different cases used in the present study for a square porous cavity

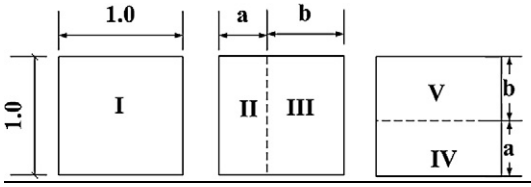

$(a + b = 1.0)$

Cases	Region	Porosity	a	b
Case 0	I	0.4	–	–
Case 1	II	0.4	0.25	–
	III	0.04	–	0.75
Case 2	II	0.4	0.5	–
	III	0.04	–	0.5
Case 3	II	0.4	0.75	–
	III	0.04	–	0.25
Case 4	IV	0.4	0.25	–
	V	0.04	–	0.75
Case 5	IV	0.4	0.5	–
	V	0.04	–	0.5
Case 6	IV	0.4	0.75	–
	V	0.04	–	0.25

Table 2
Validation of the numerical code in the case of pure thermal convection ($N = 0$) for Darcy model and $Le = 10$

Ra	Nu			Sh		
	Trevisan and Bejan [4]	Goyeau et al. [9]	Present study	Trevisan and Bejan [4]	Goyeau et al. [9]	Present study
100	3.27	3.11	3.05	15.61	13.25	12.93
200	5.61	4.96	4.85	23.23	19.86	19.42
400	9.69	7.77	7.59	30.73	28.41	28.9
1000	–	13.47	13.16	–	48.32	48.21
2000	–	19.9	19.48	–	69.29	70.45

Table 3
Accuracy test with $Ra = 2 \times 10^3$, $Le = 10$, case 0 ($\varepsilon = 0.4$), $N = 2$ at steady state (grid stretching parameter = 1.15)

Nodes	Present model	
	Nu_{right}	Sh_{right}
24 × 24	0.163	0.902
44 × 44	0.161	0.677
64 × 64	0.160	0.592
84 × 84	0.159	0.590

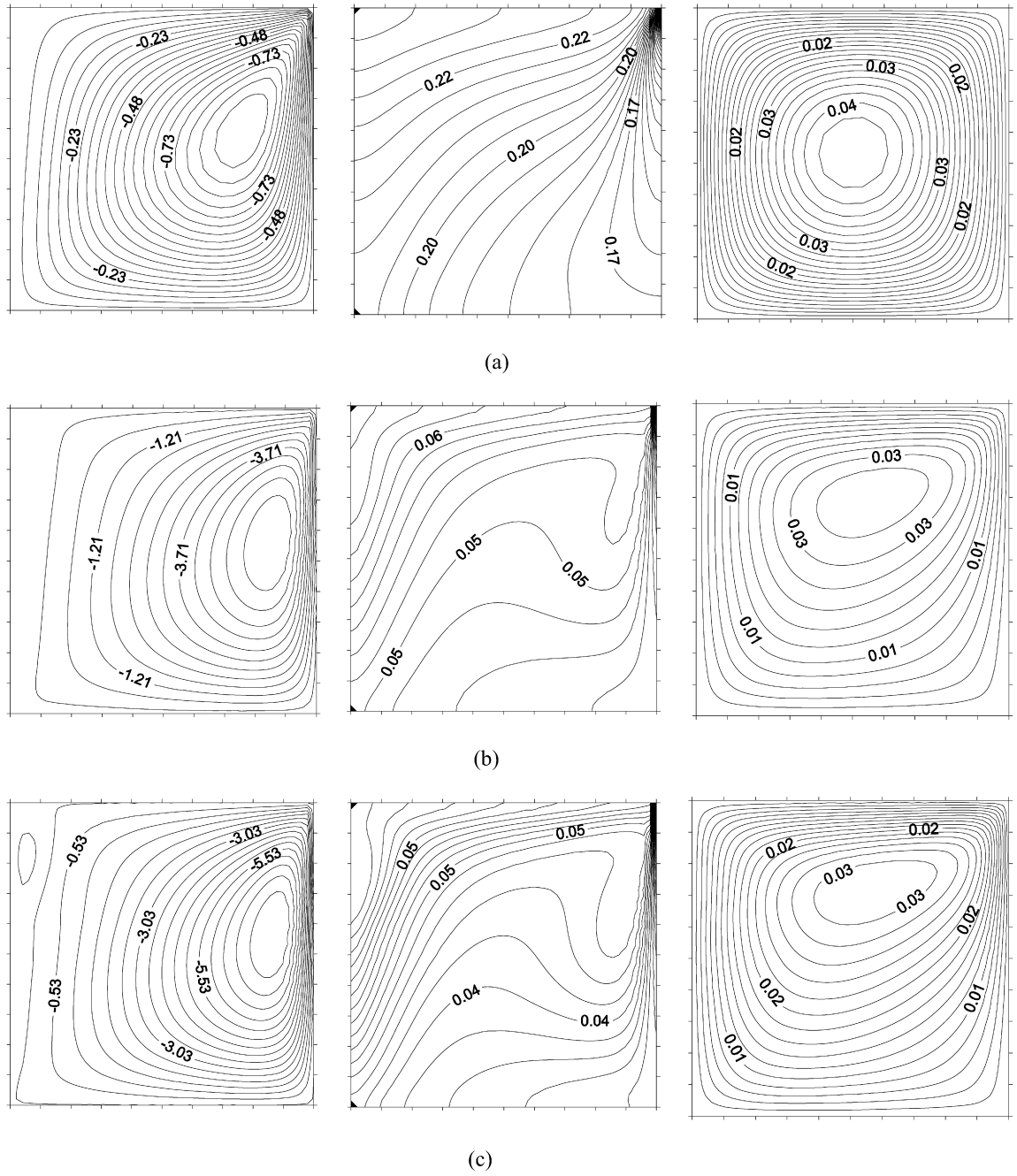

Fig. 2. Streamlines, isoconcentration lines and isotherms for $Le = 10$, $N = 2$, case 0 and (a) $Ra = 10^2$, (b) $Ra = 3 \times 10^3$, (c) $Ra = 5 \times 10^3$.

$$\frac{\partial^2 \Psi}{\partial X^2} + \frac{\partial^2 \Psi}{\partial Y^2} = -Ra\left(\frac{\partial \theta}{\partial X} + N\frac{\partial C^*}{\partial X}\right) \tag{10}$$

$$\sigma\frac{\partial \theta}{\partial \tau} + U\frac{\partial \theta}{\partial X} + V\frac{\partial \theta}{\partial Y} = \frac{\partial^2 \theta}{\partial X^2} + \frac{\partial^2 \theta}{\partial Y^2} + (1-\varepsilon) \tag{11}$$

$$\varepsilon\frac{\partial C^*}{\partial \tau} + U\frac{\partial C^*}{\partial X} + V\frac{\partial C^*}{\partial Y} = \frac{1}{Le}\left(\frac{\partial^2 C^*}{\partial X^2} + \frac{\partial^2 C^*}{\partial Y^2}\right) + \frac{(1-\varepsilon)}{Le} \tag{12}$$

where $Ra = \frac{Kg\beta_T L\Delta T}{\nu\alpha}$, $N = \frac{\beta_C \Delta C}{\beta_T \Delta T}$, $Le = \frac{\alpha}{D}$ and $\sigma = \frac{\varepsilon(\rho c_p)_f + (1-\varepsilon)(\rho c_p)_s}{(\rho c_p)_f}$.

The initial and boundary conditions for Eqs. (10), (11) and (12) are as follows:

$$\begin{aligned}
&\tau = 0: \quad \Psi = 0,\ C^* = 0,\ \theta = 0 \text{ at everywhere}\\
&\tau > 0: \quad \Psi = 0,\ \frac{\partial C^*}{\partial Y} = 0,\ \theta = 0,\ Y = 0, 1\\
&\tau > 0: \quad \Psi = 0,\ \frac{\partial C^*}{\partial X} = 0,\ \theta = 0,\ X = 0
\end{aligned} \tag{13}$$

In addition, the boundary condition for partially permeable wall can be written as follows:

$$\begin{aligned}
&\tau > 0: \quad \Psi = 0,\ \frac{\partial C^*}{\partial X} = 0,\ \theta = 0 \text{ at } X = 1 \text{ for } 0 \leqslant Y \leqslant A\\
&\tau > 0: \quad \Psi = 0,\ C^* = 0,\ \theta = 0 \text{ at } X = 1 \text{ for } A < Y < 1.0
\end{aligned} \tag{14}$$

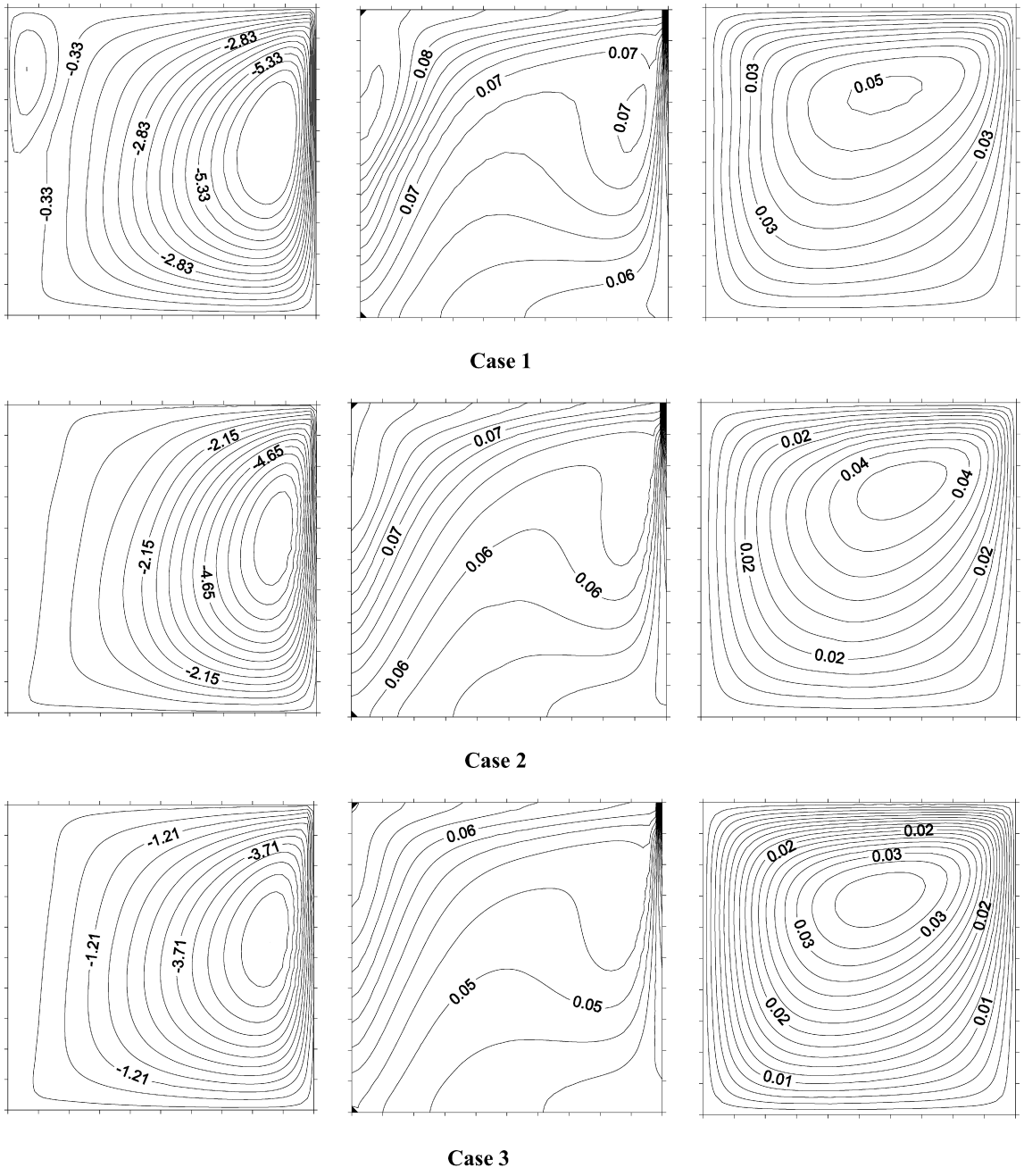

Fig. 3. Streamlines, isoconcentration lines and isotherms for $Le = 10$, $N = 2$ and $Ra = 3 \times 10^3$.

where $A = L_a/L$ and A is 0.75. The value of the streamfunction over such a boundary condition is considering as constant. It is assumed that the mass transfer through the walls is small enough in order to validate the use of zero normal velocity values at the walls, Costa [12]. The average Nusselt and Sherwood numbers at the partially permeable wall are given as:

$$Sh = -\int_A^1 \frac{\partial C^*}{\partial X}\,\mathrm{d}Y, \qquad Nu = -\int_0^1 \frac{\partial \theta}{\partial X}\,\mathrm{d}Y \tag{15}$$

In this investigation, particularly, the problem was solved for a homogenous porous medium and its porosity is 0.4 everywhere in the cavity. Then, it was considered that the cavity had two regions with different porosity. All these different cases were shown schematically in Table 1. In these cases, the porosity of the medium has two values as $\varepsilon_1 = 0.4$ and $\varepsilon_2 = 0.04$.

3. Solution procedure

The governing equations were discretized using the finite volume method of Patankar [17]. The grid layout was arranged by utilizing collocated grid procedure, while the power law-differencing scheme was adopted for heat and mass fluxes in the fluid domain. The iterative procedure was performed with the

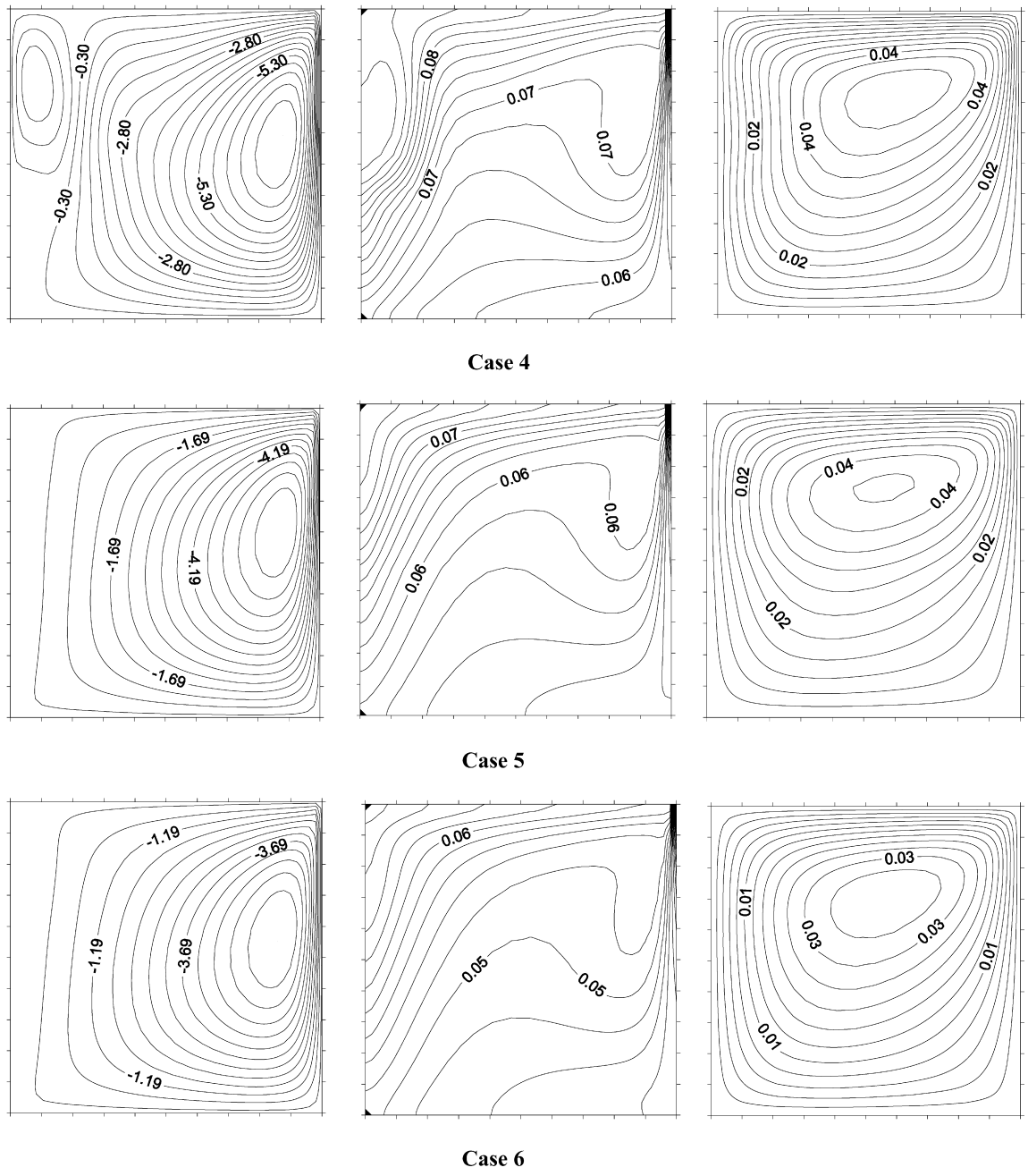

Fig. 4. Streamlines, isoconcentration lines and isotherms for $Le = 10$, $N = 2$ and $Ra = 3 \times 10^3$.

Alternating Direction Implicit method (ADI). The streamfunction field is calculated by using a Successive Over Relaxation method (SOR). The iteration process was terminated under the following condition:

$$\sum_{i,j} \left|\lambda_{i,j}^{n} - \lambda_{i,j}^{n-1}\right| / \sum_{i,j} \left|\lambda_{i,j}^{n}\right| \leqslant 10^{-5} \tag{16}$$

where λ is the general dependent variable which can stands for Ψ, θ, C^* and n denotes the iteration step. The suitable dimensionless time step $\Delta\tau$ was 10^{-3} in this investigation for all Darcy modified Rayleigh numbers. For benchmarking purpose, the accuracy of the numerical code was checked in the case of double diffusive convection within a differentially heating square porous enclosure subject to a concentration difference, ΔC and a temperature difference, ΔT in the horizontal direction using the results reported in Trevisan and Bejan [4], Goyeau et al. [9]. The results presented in Table 2 concern mass transfer due to purely thermal natural convection ($N = 0$) for Darcy model. It can be seen from Table 2 that the average *Nu* and *Sh* numbers are in good agreement with those published in the references. Accuracy tests were also performed the present mathematical model ($N = 2$) at steady state using four sets of grids as shown in Table 3. The results show insignificant difference between the 64×64 and 84×84. A non-uniform grid (64×64) was used in all calculations.

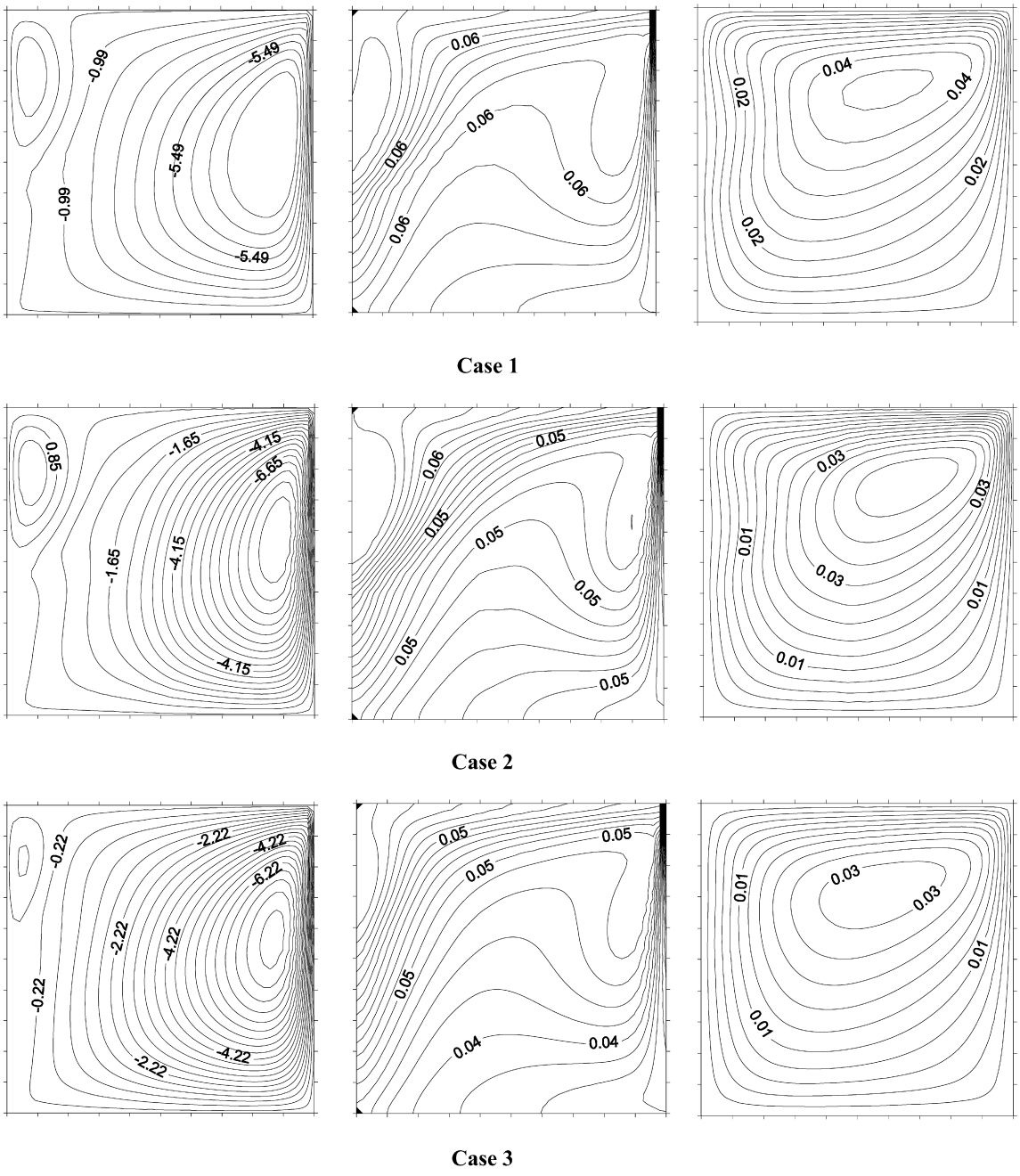

Fig. 5. Streamlines, isoconcentration lines and isotherms for $Le = 10$, $N = 2$ and $Ra = 5 \times 10^3$.

4. Results and discussion

The buoyancy ratio and Lewis number were held fixed throughout this investigation ($N = 2$ and $Le = 10$). The results were presented for Darcy modified Rayleigh number range 10^2–5×10^3 and for seven different cases as explained in Table 1. The results presented here are based on the steady-state results obtained from the transient solutions of Eqs. (10)–(12) subject to the boundary conditions given by Eqs. (13) and (14). The streamlines, isoconcentration lines and isotherms for $Le = 10$, $N = 2$ and case 0 ($\varepsilon = 0.4$) at different Darcy modified Rayleigh numbers were presented in Fig. 2. As seen in Fig. 2, as Darcy modified Rayleigh number increases the velocity of fluid and the temperature gradients increase. The velocity of fluid is higher at the right wall near the permeable part; therefore the streamlines crowd near the top of the right wall and it is observed a clockwise rotating cell through the right wall. As Darcy modified Rayleigh number increases, the natural convection increase, the boundary layer thickness decreases due to the higher velocity gradient near the right wall in Fig. 2. Also, the concentration gradients crowd near the top of the right wall for all Darcy modified Rayleigh numbers because of the permeable section of the wall. The crowded gradients show that buoyancy effect due to mass transfer and the natural convection is dominant at this region as seen in Fig. 2. Figs. 3 and 4 show the streamlines, isoconcentration lines and isotherms at $Ra = 3000$

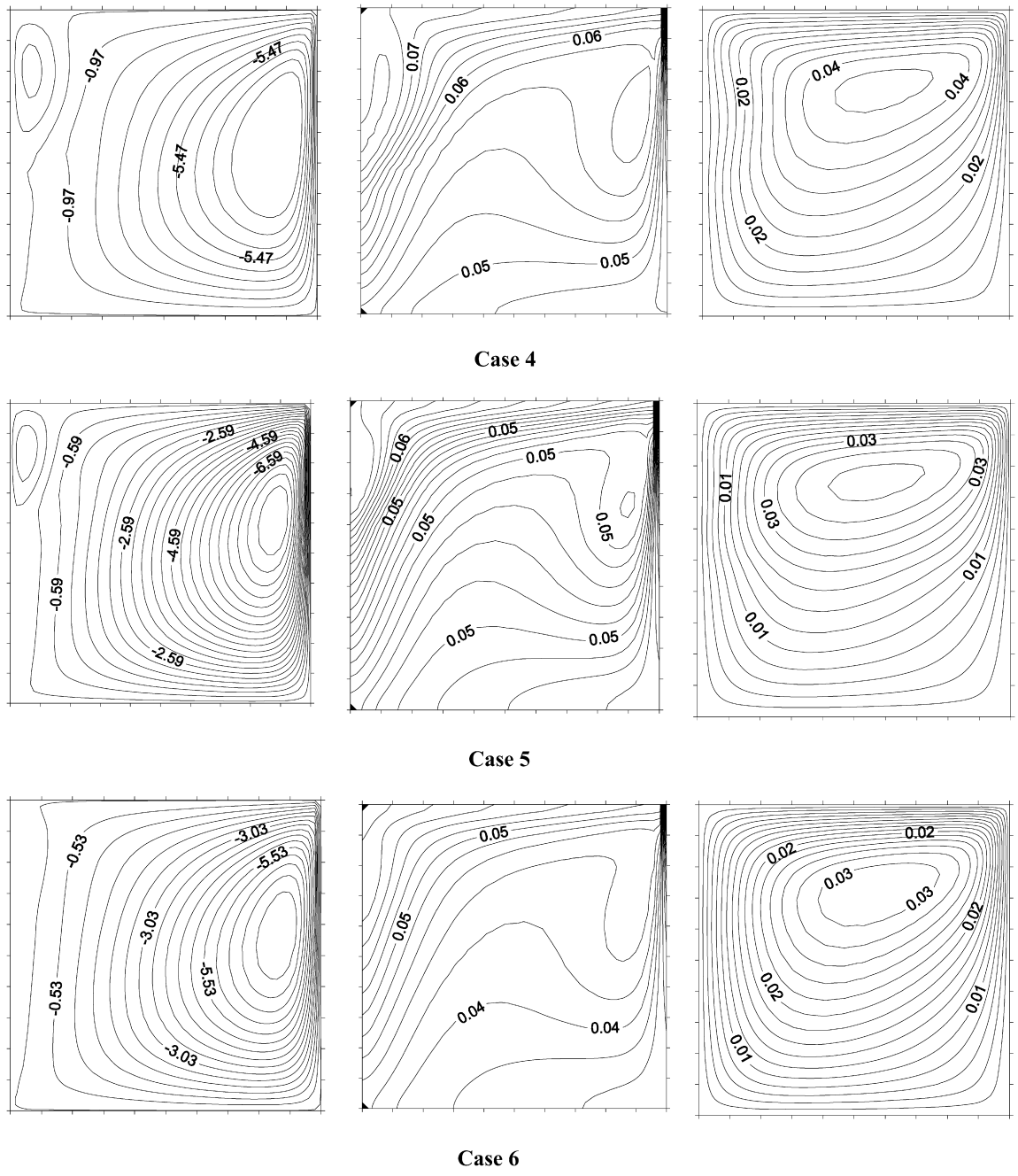

Fig. 6. Streamlines, isoconcentration lines and isotherms for $Le = 10$, $N = 2$ and $Ra = 5 \times 10^3$.

for all cases except case 0. In Figs. 3 and 4, a counter clockwise secondary cell occurs in the streamlines at the upper left of the cavity for case 1 and case 4. Also as seen in Figs. 2(b), 3 and 4, the isoconcentration lines are considerably different from case 0 at case 1 and case 4. The concentration gradients are higher at the upper left of the cavity for case 1 and case 4. The temperature gradients crowd at the top of the right wall for all cases as seen in Figs. 3 and 4. The streamlines, isoconcentration lines and isotherms at $Ra = 5000$ for all cases except case 0 were presented in Figs. 5 and 6. As illustrated in Figs. 2(c), 5 and 6, the isoconcentration lines and streamlines show considerably changes at cases 1, 2, 4 and 5, in these cases the porosity of the medium is 0.04 in 50 percentage (cases 2 and 5) and in 75 percentage (cases 1 and 4). The second counter clockwise rotating cell occurs in the streamlines at the upper left of the cavity for all cases except case 6 as seen in Figs. 5 and 6. The concentration gradients crowd not only at the top of the right wall but also at the left upper part of the cavity especially in case 2 and case 5. The streamlines crowd near the permeable part of the right wall and also the main clockwise rotating cell occurs near the right wall and the concentration and temperature are higher at the top of the cavity for all cases as seen in Figs. 3 to 6, respectively.

The average Sherwood number versus different Darcy modified Rayleigh numbers was given for the permeable part of the right wall in Fig. 7(a). *Sh* number nearly equals for cases 0, 3

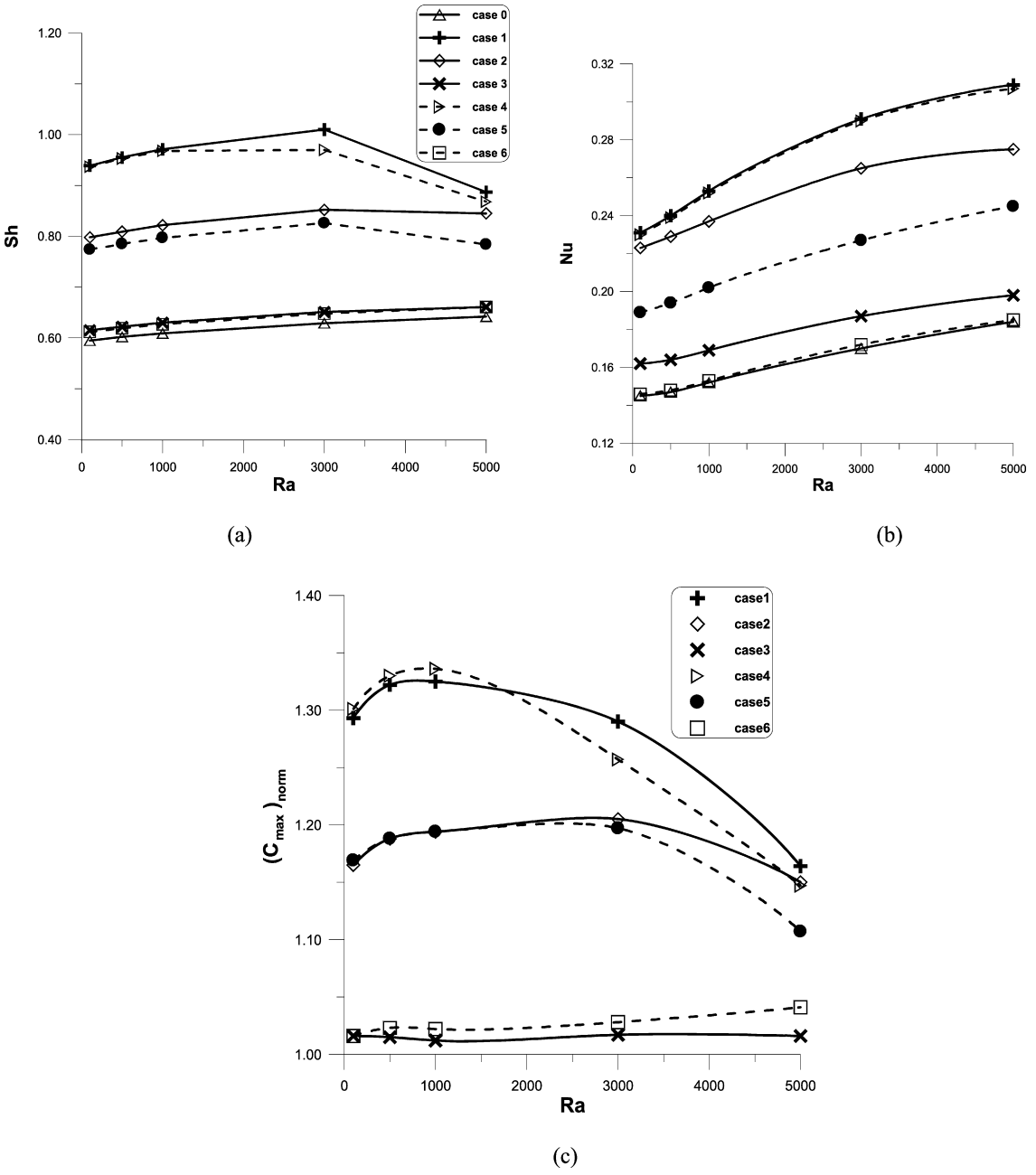

Fig. 7. For all cases, at $Le = 10$, $N = 2$, (a) Average Sh number, (b) *Nu* number and (c) Normalized concentration, $(C_{\max})_{\text{norm}} = (\frac{C_{\max}}{(C_{\max})_{\text{case 0}}})$ depending of *Ra* number.

and 6, however it is higher values for cases 1, 2, 4 and 5 and *Sh* number decreases after $Ra = 3000$ in these cases as seen in Fig. 7(a). Also, the average Nusselt number versus Darcy modified Rayleigh number was given for the right wall in Fig. 7(b). The average *Nu* number increases as Darcy modified Rayleigh number increases for all cases. The average *Nu* number nearly equals for cases 1 and 4 and for cases 0 and 6. *Sh* and *Nu* numbers have higher values for cases 1, 2, 4 and 5 compared to case 0, also the maximum concentration and temperature gradients occur at cases 1 and 4 as seen in Fig. 7(a) and (b).

The normalized concentration depending on different Darcy modified Rayleigh numbers was given in Fig. 7(c). The normalized concentration is the ratio of the maximum concentration in the cavity between any case and case 0. The normalized concentration increases from case 3 to case 1 for the same Darcy modified Rayleigh number, that is the concentration in all cases is higher than that the case 0. As a result, the leakage from the cavity decreases in all cases compared to case 0 as seen in Fig. 7(c). On the other hand, the normalized concentration decreases for $Ra > 1000$ for cases 1 and 4 and for $Ra > 3000$ for cases 2 and 5 as seen in Fig. 7(c). In these cases, as Darcy modified Rayleigh increases the leakage from the cavity increases as well. The value of the normalized concentration for cases 3 and 6 is almost same that of case 0.

The dimensionless temperature and concentration profiles at the horizontal mid-plane of the cavity for $Ra = 5 \times 10^3$ were

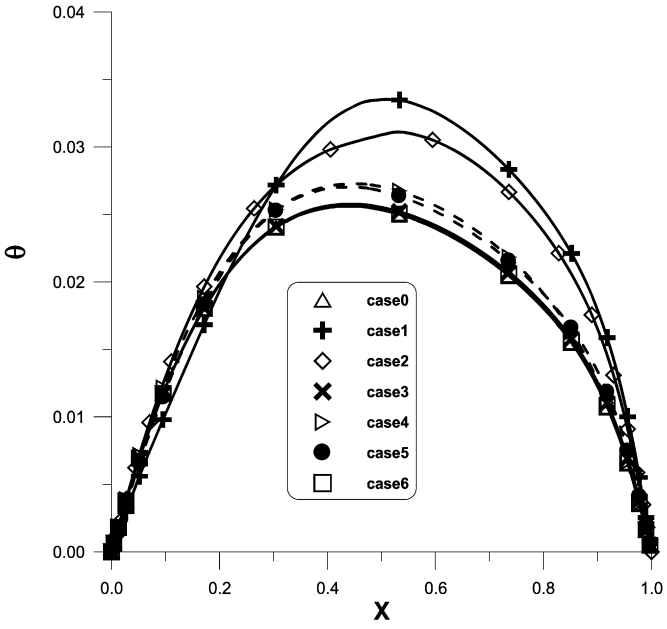

(a)

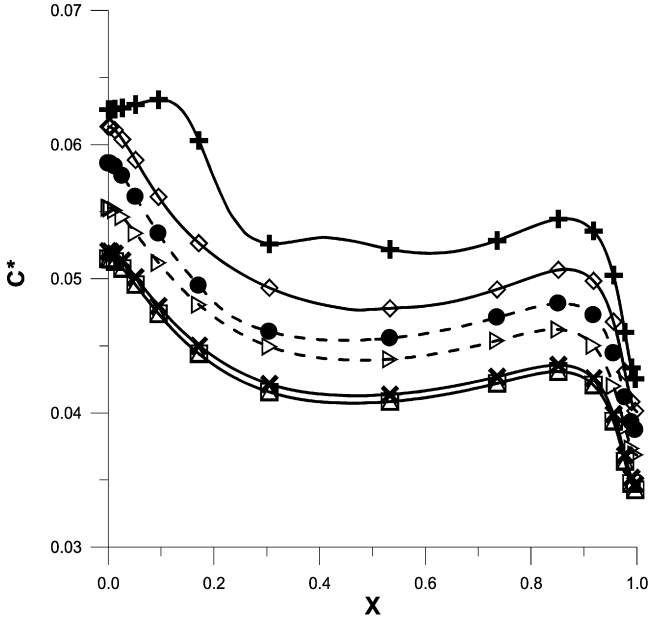

(b)

Fig. 8. The dimensionless temperature and concentration profiles at the horizontal midplane of the cavity for $Ra = 5 \times 10^3$.

given in Fig. 8. As seen Fig. 8(a), the dimensionless temperature profiles are similar for case 0-case 3-case 6 and for case 4-case 5 and the maximum of the profiles are almost at $X = 0.4$. But the dimensionless temperature profiles have different and higher values for case 1 and case 2, also the maximum of the profiles is almost at $X = 0.6$ in these cases. Since, the right region of the cavity has lower porosity in these cases, the maximum temperature occurs through the right side of the cavity. The dimensionless concentration of the left side is greater than that of the right side because of the leakage from the partially permeable right wall as seen in Fig. 8(b). The dimensionless concentration profiles are same for case 0, case 3, and case 6. However, they have different and higher values for cases 1, 2, 4 and 5 as indicated in Fig. 8(b). In addition, the dimensionless concentration has higher values in the cases which the porosity is 0.4 in the left region of the cavity (cases 1 and 2) compared to the cases which the porosity is 0.4 in the bottom region of the cavity (cases 4 and 5).

5. Conclusions

The problem of double-diffusive natural convection in a porous cavity filled with a mass-producing and heat-generating solid phase and with partially permeable right wall has been analyzed by using different porosity cases in the presented study. The main findings of this investigation are as follows:

The temperature and concentration gradients in all cases are larger according to the medium with homogenous porosity. Case 3 and case 6 behave like case 0 in general, since the porosity of the medium is 0.4 in 75 percentage in these cases. The maximum leakage from the cavity is at case 0 (homogenous case). The amount of the solid phase is similar in the case 1 and case 4. However, the amount of the leakage from the cavity for case 4 is higher than for case 1 for high Darcy modified Rayleigh numbers as seen in Figs. 7(c) and 8(b). The similar situation is valid for case 2 and case 5, so the leakage from the cavity is higher in the case 5 for high Darcy modified Rayleigh numbers. As a result, the leakage from the cavity has higher values in the cases that the porosity of the bottom region of the cavity is 0.4 (case 4 and case 5) for high Darcy modified Rayleigh numbers.

References

[1] D.A. Nield, A. Bejan, Convection in Porous Media, second ed., Springer-Verlag, New York, 2006.
[2] D.B. Ingham, I. Pop (Eds.), Transport Phenomena in Porous Media, Pergamon, Oxford, 1998.
[3] I. Pop, D.B. Ingham, Convective Heat Transfer: Mathematical and Computational Modelling of Viscous Fluids and Porous Media, Pergamon, Oxford, 2001.
[4] A. Trevisan, O.V Bejan, Natural convection with combined heat and mass transfer buoyancy effects in a porous medium, International Journal of Heat and Mass Transfer 28 (1985) 1597–1611.
[5] D. Angirasa, G.P. Peterson, I. Pop, Combined heat and mass transfer by natural convection with opposing buoyancy effects in a fluid saturated porous medium, International Journal of Heat and Mass Transfer 40 (1997) 2755–2773.
[6] C. Béghein, F. Haghighat, F. Allard, Numerical study of double-diffusive natural convection in a square cavity, International Journal of Heat and Mass Transfer 35 (1992) 833–846.
[7] S. Akbal, A.F. Baytas, Numerical analysis of gas transfer by natural convection in a fluid saturated porous medium, in: R. Bennacer, A.A. Mohamad, M. El-Ganaoui, J. Sicard (Eds.), Proc. of 4th ICCHMT: Progress in Computational Heat and Mass transfer, 2005, pp. 313–315.
[8] J.H. Merkin, T. Mahmood, Convective flows on reactive surfaces in porous media, Transport in Porous Media 33 (1998) 279–293.
[9] B. Goyeau, D. Songbe, J.-P. Gobin, Numerical study of double-diffusive natural convection in a porous cavity using the Darcy–Brinkman formu-

lation, International Journal of Heat and Mass Transfer 39 (1996) 1363–1378.
[10] M. Bourich, A. Amahmid, M. Hasnaoui, Double diffusive convection in a porous enclosure submitted to cross gradients of temperature and concentration, Energy Conversion and Management 45 (2004) 1655–1670.
[11] A. Bahloul, L. Kalla, R. Bennacer, H. Beji, P. Vasseur, Natural convection in a vertical porous slot heated from below and with horizontal concentration gradients, International Journal of Thermal Sciences 43 (2004) 653–663.
[12] V.A.F. Costa, Double diffusive natural convection in a square enclosure with heat and mass diffusive walls, International Journal of Heat Mass Transfer 40 (1997) 4061–4071.
[13] D. Gobin, B. Goyeau, A.A. Neculae, Convective heat and solute transfer in partially porous cavities, International Journal of Heat and Mass Transfer 48 (2005) 1898–1908.
[14] A.K. Singh, T. Paul, G.R. Thorpe, Natural convection due to heat and mass transfer in a composite system, Heat and Mass Transfer 35 (1999) 39–48.
[15] E. David, G. Lauriat, P. Cheng, A numerical solution of variable porosity effects on natural convection in a packed-sphere cavity, Journal of Heat Transfer Transactions of the ASME 113 (1991) 391–399.
[16] Z.M. Saghir, R.M. Islam, Double diffusive convection in dual-permeability, dual-porous media, International Journal of Heat and Mass Transfer 42 (1999) 437–454.
[17] S.V. Patankar, Numerical Heat Transfer and Fluid Flow, Hemisphere/McGraw–Hill, Washington, DC, 1980.